Available online at www.sciencedirect.com

ScienceDirect

IFAC PapersOnline CONFERENCE PAPER ARCHIVE

IFAC PapersOnLine 58-28 (2024) 31–36

The cost of transition: modeling the swimming biomechanics of bottlenose dolphins to estimate cost of transport ⋆

Ningshan Wang * **Gabriel Antoniak** * **Kira Barton** *
Nicole West ** **K. Alex Shorter** *

* *University of Michigan, Ann Arbor, MI, USA (Corresponding author's email: kshorter@umich.edu).*
** *Dolphin Quest Oahu, Honolulu, HI, USA*

Abstract: Given growing interest in emulating dolphin morphology and motion gait to design bio-inspired underwater vehicles with high performance, this article investigate bottlenose dolphin (Tursiops truncatus) swimming behavior using tag-measured kinematics and a hydrodynamic model to estimate propulsive power, and energetic cost of transport. This article investigated the energetic costs associated with transient behavior required to reach steady state, i.e. additional costs required to reach steady state swimming speeds. To this end, movement data were collected from three animals during prescribed straight-line swimming trials to investigate swimming mechanics. The swimming speed ranges from 2m/s-5 m/s and the thrust power range from 0.1kw-1.5 kw. 239 qualified active-fluking periods were manually segmented and 277 qualified consistent-speed periods were automatically segmented from the collected dataset. A velocity-dependent hydrodynamic model to calculate propulsion efficiency from prior research is employed to calculate energetic costs of individual animals. These results provides new insights into dolphin swimming behavior in prescribed trial-swimming tasks and presents a path forward for continuous estimates of mechanical work and power from wild animals.

Keywords: Biomechanics, hydrodynamics, bio-tagging, system/model identification

1. INTRODUCTION

Efficient movement through the water is important for biological and engineered systems. Current literature indicates that cetaceans (orcas, dolphins, and whales), may be more efficient across their range of thrust production than engineered propellers. For ceteaceans, propulsive efficiencies have been estimated to reach as high as 90%, and may maintain efficiencies above 80% across their entire range of speeds. In contrast, propellers are around 70% at their most efficient point. Cetaceans also produce about four times more thrust than mechanical propellers for the power exerted (Fish and Lauder, 2006). However, the mechanisms behind efficient movement of underwater biological systems are not well understood, in part because the kinematic information in a wild and free-swimming environment is limited to animal kinematics.

In managed marine environments, kinematic data extracted from camera data have been used to supplement kinematic measurements. For bottlenose dolphins, existing research has combined measured speed and kinematics of the fluke (amplitude, frequency, angle of attack) with hydrodynamic models to estimate external forces acting on the animals, such as drag and thrust (Fish, 1993; Fish and Rohr, 1999; Schultz and Webb, 2002). Particle image velocimetry has also been used to estimate thrust created by swimming bottlenose dolphins (Fish et al., 2014). More recently, per-stroke thrust and power has been studied with a Pacific white-sided dolphin in high-speed propulsion using camera-based tracking and drag estimates from computational models (Tanaka et al., 2019). However, because these approaches use video data to measure kinematics the analysis is limited to a few strokes when the animal is in the camera's field of view. As such, there currently exists a significant gap in our knowledge about the mechanical work performed by dolphins during extended periods of swimming and daily life.

The studies on cetacean swimming dynamics are challenging, because the animals spend a significant portion of their active time underwater and out of visual range. Moreover, most of the cetaceans oscillate their fluke through the water to propel in the marine environment. The lift-based thrust force and drag force acted on the moving body are hardly feasible for direct measurement. A reliable solution to this challenge is the bio-logging tag. Bio-logging tags (Gabaldon et al., 2022) that collect kinematic data (speed, acceleration, position at the surface, orientation, depth) enable the researchers to measure high resolution movement data in managed and wild settings. Although animal kinetics can not be directly measured with these systems, we can infer the mechanical work and power from these measurements by leveraging the hydro-dynamic model based on kinematic information. Tag-based kinematic measurements of animal movement provide new in-

⋆ This work was supported by a Contribution Agreement with the Department of Fisheries and Oceans Canada (DFO), and the National Science Foundation under Grant No. 2238432.

10.1016/j.ifacol.2024.12.006

sights into the energetic cost, swimming gait and behavior of the animals.

Modeling approaches that use kinematic measurements from bio-logging tags to estimate swimming kinetics are key to the investigation of cetacean swimming biomechanics. A common approach has been to estimate energetic costs of swimming using proxies such as overall dynamic body acceleration (Wilson et al., 2006). This approach has been developed and tested with terrestrial animals and free-diving sea lions where direct measurements of metabolic cost via respirometry have been possible (Fahlman et al., 2008; Halsey et al., 2009; Wilson et al., 2006, 2020). Experimental validation of the relationship between acceleration, mechanical work, and energetic cost remains limited for free-swimming cetaceans (Van Der Hoop et al., 2014; Williams et al., 1993; Yazdi et al., 1999). Without calibration (which is seldom possible on large marine animals), comparisons between individuals are unlikely to be accurate and comparisons across different behaviors within an individual may not hold. To date, most existing research has focused on bio-mechanics during steady state swimming where animals use a continuous fluking-gait to maintain their speed through the water. These studies indicate that animals modulate consistent-speed (CS) swimming speed by increasing fluking frequency but not amplitude (Fish, 1993). Further, animals select average swimming speeds that minimize steady state cost of transport (COT) (Gabaldon et al., 2022). However, these studies have not included costs associated with transient behavior required to reach steady state or to move between swimming speeds.

In this article, we leveraged the kinematic data from biologging tags and a physics based modeling approach to investigate the additional cost required to accelerate the animal from rest to steady state swimming speeds during a prescribed swimming task. Working with the team at Dolphin Quest Oahu, animals were trained to wear biologging tags and swim across their lagoon environment over a range of speeds. Laps were segmented into periods of active fluking (AF) that were autonomously identified using features in the kinematic data recorded by the tag. Periods of consistent-speed (CS) swimming were identified during AF period. Animal acceleration and speed measurements were used with a model of the drag force acting on the animal to estimate propulsive thrust, thrust power, and COT during the trials. Average thrust power and COT calculated during both AF and CS periods to investigate the additional costs required to accelerate the animal to steady state. New knowledge about these transient periods of movement will lead to a better understanding of ceteacean swimming biomechanics, and is an important step towards the experimental validation of the relationship between acceleration, mechanical work, and energetic cost for free-swimming cetaceans (Van Der Hoop et al., 2014; Williams et al., 1993; Yazdi et al., 1999).

2. MATERIALS & METHODS

2.1 Data collection

Experiments were conducted at Dolphin Quest Oahu, HI, with three bottlenose dolphins (*Tursiops truncatus*).The dolphins were trained by the animal care specialists to perform a controlled swimming task while wearing biologging tags (MTags) placed between the blow hole and dorsal fin. Each lap started with the animal stationed at a floating dock, Fig. 2. The animals then swam, underwater, around an animal care specialist at the far side of the lagoon and back to the floating dock. Lap distances were typically 35 m long (around 70 m out and back), and the animals were trained to swim over a range of speeds. Depth, pitch angle, forward acceleration and speed in body-fixed reference frame were used to identify swimming events and to calculate the estimated thrust force during the trials.

MTags are persistently monitoring biologging tags with internal electronics built on the OpenTag3 platform (Loggerhead Instruments, Sarasota, FL, USA). Kinematic sensors include: 3-axis accelerometer, 3-axis magnetometer, 3-axis gyroscope, temperature sensor and pressure sensor. Forward water speed was measured using a secondary circuit board with a 1-axis Hall-effect sensor, and a free-spinning uni-axial magnetic micro-turbine mounted in line with the tag fin. The tag attached to the animal for experiment is presented in Fig 1.

Measurements of acceleration, geo-magnetism and angular velocity were sampled at 50 Hz and further filtered using Madgwick filter (Madgwick et al., 2010) to estimate orientation (pitch, roll, and heading). The depth and forward-speed were sampled at 5Hz from the pressure sensor and turbine flow sensor and filtered using the method presented in (Gabaldon, 2021, Chapter 3).

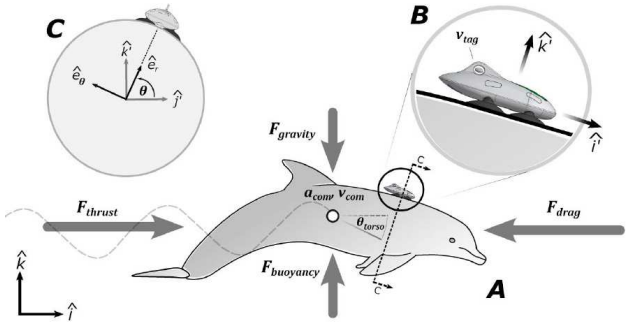

Fig. 1. An illustration of the simplified forces acting on the animal during swimming, as well as kinematic parameters measured by the tag.

2.2 Swimming dynamics

Estimated thrust power was calculated using the approach presented in (Gabaldon et al., 2022). We assumed that the animal can control buoyancy to balance the gravitational force acting on the body, and combined the remaining forces into net thrust and net drag. With balanced vertical motion of the animals, we model the longitudinal motion of the animals by:

$$m' a_{\text{com}} = F_{\text{thrust}} + F_{\text{drag}}, m' = m + m_{\text{add}}, \qquad (1)$$

where m' is the total effective mass and a_{com} is the center-of-mass (COM) acceleration of the animal. This total effective mass is defined by the mass of the animal m plus the added mass of fluid (Fossen, 2011) displaced by the animal during movement. (Weihs, 2002) modeled the

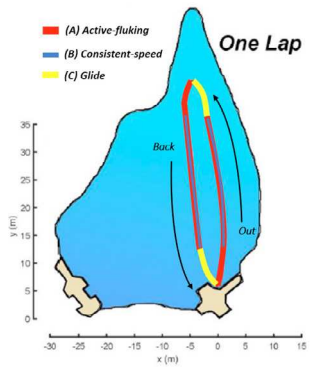

(a) Trail-swimming map

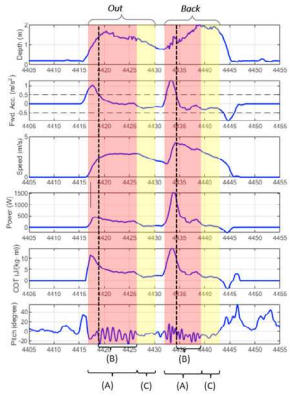

(b) An illustration of the lagoon environment at Dolphin Quest Oahu. The MTag measurements and estimations of a swimming trial

Fig. 2. (*Top*) A round-trip swimming trial is segmented into three periods of three types, which are A) active-fluking B) consistent-speed C) glide. (*Bottom*) Measurements of depth, forward-acceleration, speed and torso pitching angle, during round-trip swimming trial. Estimates of power and cost of transport during round-trip swimming trial. Swimming periods are highlighted.

added-mass for a swimming animal by $m_{\text{add}} = 0.2\beta\rho V$, where $\rho = 1030\text{kg/m}^3$ is the density of seawater and V is the displacement volume of the animal by 3D modeling. β is the ratio of drag force during active swimming versus gliding. (Weihs, 2002) used the functional range of $1 < \beta < 3$. As explicit values of β are not known for these dolphins and swimming conditions, we operates with the assumption of $\beta = 2$ as a conservative estimate, such that $m_{\text{add}} = 0.4\rho V$. Thrust power P_{thrust} is calculated by the product of thrust force F_{thrust} and COM velocity v_{com} such that $P_{\text{thrust}} = F_{\text{thrust}} v_{\text{com}}$. Thereafter, we obtain the thrust power of swimming expressed as follows:

$$P_{\text{thrust}} = F_{\text{thrust}} v_{\text{com}} = m' a_{\text{com}} v_{\text{com}} - F^{\dagger}_{\text{drag}} v_{\text{com}}. \quad (2)$$

We leveraged the water-velocity v_{tag} collected from MTag to estimate v_{com} and a_{com}, where a_{com} was approximated by finite-difference of v_{tag} and smoothed by a 2-second moving-average process to reduce noise. By applying the depth-dependent drag model (Gabaldon et al., 2022) defined by:

$$F^{\dagger}_{\text{drag}} = -\frac{1}{2}\rho A_s C_D \gamma v^2_{\text{com}}, \quad (3)$$

where γ is the depth-dependent coefficient (Hertel, 1966) to account the wave drag when the animal swims close to the surface. Normalized drag coefficients were obtained by applying the relation $C_D = 16.99\text{Re}^{-0.47}$ (Fish et al., 2014), where Re is the body-length Reynolds number defined by $\text{Re} = L v_{\text{com}}/\nu$. L is animal body-length and $\nu = 1.044 \times 10^{-6}\text{m}^2/\text{s}$ is the kinematic viscosity of sea water. In (3), A_s denotes the surface area, given by $A_s = 0.08m^{0.65}$, where m is the animal mass (Fish, 1993). Finally, we obtain the expression of thrust power:

$$P_{\text{thrust}} = m' a_{\text{com}} v_{\text{com}} + \frac{1}{2}\rho A_s C_D \gamma v^3_{\text{com}}. \quad (4)$$

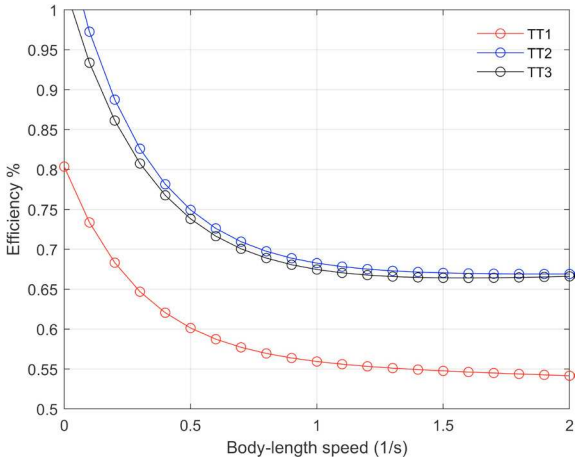

Fig. 3. Body-length speed vs velocity-dependent fluking-thrust efficiency for TT1-3. (Xargay et al., 2023; Antoniak et al., 2023)

A non-dimensional form of thrust power was calculated to compare animals with different lengths and masses,

$$P_{\text{t,nd}} = P_{\text{thrust}}/(mg^{1.5}L^{0.5}). \quad (5)$$

Both thrust power and non-dimensional thrust power were assumed to be positively correlated with the swimming speed. Thrust power and swimming speed were correlated by the following equation,

$$\begin{aligned} \widehat{P}_{\text{thrust}}(v_{\text{com}}) &= a_1 v^{a_2}_{\text{com}}, \\ \widehat{P}_{\text{t,nd}}(v_{\text{com}}) &= a^*_1 (v_{\text{com}}/L)^{a^*_2} = a^*_1 v^{a^*_2}_{\text{bl}}, \end{aligned} \quad (6)$$

where v_{bl} is the individual body-length speed, and a_1, a_2, a^*_1, a^*_2 are positive scalars to be determined using a nonlinear curve-fitting process.

To provide predictions for the animals' metabolic power, work, and cost of transport, additional factors must be considered. To account for the energy loss as chemical energy is converted into mechanical energy, the mammalian metabolic-to-muscle power efficiency (chemical) was taken to be $\eta_{\text{ms}} = 0.25$ according to (Massaad et al., 2007). The efficiency between the internal power used to move the fluke through the water and the resulting external propulsive power was denoted as η_{sp} in this article. In prior research (Gabaldon, 2021; Gabaldon et al., 2022), this fluking-to-propulsion power efficiency was selected to be $\eta_{\text{sp}} = 0.85$ according to (Fish, 1998). In this article, we consider a η_{sp} that changes with the animal's swimming speed (v_{com}) according to the fluking efficiency model from (Xargay et al., 2023; Antoniak et al., 2023). This approach was used to identify animal specific efficiencies that were model $\eta_{\text{sp}}(v_{\text{com}})$ by

$$\eta_{\text{sp}}(v_{\text{com}}) = c_1 e^{c_2 v_{\text{com}}} + c_3 v_{\text{com}} + c_4. \quad (7)$$

Fig. 3 presents the relationship between body-length speed and fluking efficiency of animals TT1 - TT3 that participated in this article. The coefficients c_{1-4} are presented at the bottom of Table 1 for individuals.

Thereafter, we define the energetic cost of transport by the following expression:

$$\text{COT} = \frac{P_{\text{thrust}}/(\eta_{\text{ms}}\eta_{\text{sp}}) + P_{\text{RMR}}}{m v_{\text{com}}}, \quad (8)$$

where P_{RMR} is the resting metabolic power of an animal. The method to obtain P_{RMR} is available in (Allen et al.,

2022; Gabaldon et al., 2022). We substitute the estimated thrust power $\widehat{P}_{\text{thrust}}$ given by (6) into (8) To provide continuous predictions of COT, given by:

$$\widehat{\text{COT}} = \frac{\widehat{P}_{\text{thrust}}(v_{\text{com}})/(\eta_{\text{ms}}\eta_{\text{sp}}(v_{\text{com}})) + P_{\text{RMR}}}{mv_{\text{com}}}. \quad (9)$$

Similar to the thrust power, the COT is also assumed to be correlated by swimming speed, given by:

$$\widehat{\text{COT}} = \frac{b_1 v_{\text{com}}^{b_2} + P_{\text{RMR}}}{mv_{\text{com}}}. \quad (10)$$

A COT vs body-length speed correlation is also conducted to analyze animals with different lengths and masses in cluster, given by:

$$\widehat{\text{COT}}_{\text{bl}} = \frac{b_1^* v_{\text{bl}}^{b_2^*} + \overline{P}_{\text{RMR}}}{\overline{m}\overline{L}v_{\text{bl}}}, \quad (11)$$

where $\bar{L}$, $\bar{m}$, $\bar{P}_{\text{RMR}}$ are averaged animal masses, body lengths and RMRs. In (10) and (11), b_1, b_2, b_1^*, b_2^* are positive scalars to be determined using a nonlinear curve-fitting process.

Algorithm 1 The algorithm to segment AF swimming period

```
AF = 0:                ▷ AF == 0: AF period does not start
                       ▷ AF == 1: AF period starts
Trial start
while True do
    if Depth > 0.5m & Fluctuating Pitch== True
& Fwd Acc> 0 & AF == 0 then
        AF = 1. Record the timestamp.   ▷ AF period
starts.
    end if
    if (Depth ≤ 0.5m ‖ Fluctuating Pitch== False ‖
Fwd Acc< -0.5 )& AF == 1  then
        AF = 0. Record the timestamp.   ▷ AF period
ends.
    end if
end while
```

2.3 Segmentation and identification

Periods of animal swimming with minimal speed fluctuations, defined here as consistent-speed (CS) intervals, were identified using a heuristically tuned (manually defined parameter) automated method (Gabaldon et al., 2022). Periods of animal swimming with positive thrust fluking, defined here as active-fluking (AF) intervals, were identified manually using the method presented in Algorithm 1. These two methods for segmentation are presented as follows.

Consistent-speed swimming: First, speed data v_{com} from MTag were smoothed using a 2-second Savitzky-Golay filter to produce $\overline{v}_{\text{com}}$. This filtering method was chosen for its ability to perform smoothing while preserving overall signal shape, which was useful when identifying specific time indices. A 2-second moving-window standard deviation was computed for $\overline{v}_{\text{com}}$, to produce $\sigma_{\overline{v}} = 0.045\text{ms}^{-1}$. During steady-state swimming, a dolphin would be fluking to overcome drag effects, which would result in positive P_{thrust} rather than zero during no motion, hence minimal-movement low $\sigma_{\overline{v}}$ segments were filtered out by removing segments with low thrust power. Thrust power data were also smoothed with a 2-second Savitzky-Golay filter to produce $\overline{P}_{\text{thrust}}$, for noise reduction. A dolphin was then considered to be in a steady-state swimming pattern when $\sigma_{\overline{v}} = 0.045\text{ms}^{-1}$ and $\overline{P}_{\text{thrust}} > 50\text{W}$, both thresholds heuristically determined.

Active-fluking swimming: The segmentation algorithm of AF periods is presented in Algorithm 1.

When we compare the two methods, we find that the AF periods cover the CS periods in one trial, but AF periods include longer swimming period with higher acceleration caused by fluking thrust. The relationship between AF periods and CS periods can be observed in Fig. 2.

3. RESULTS

General metrics for the conducted experiments, differentiated by animal, are reported in Table 1. Each dolphin completed between 29 (TT2) and 54 (TT1) laps across all trials, for a total of 120 laps. The power-speed relationship for each animal is presented in (4), and the curves for the individual fits are presented in Subfigs. a)-c) in Fig. 4. The non-dimensional power vs body-length speed relationship is presented in (5) and the curve for all of the animals is presented in Subfig. d) in Fig. 4. The COT-speed relationship for each animal is presented in (9), and the curves for the individual fits and overall fit are presented in Fig. 5. The curve-fitting results for both AF segments and CS segments are presented in Figs. 4 and 5. The curve-fitting coefficients are presented at the bottom of 1.

A total of 239 active fluking segments were extracted from the swimming laps, Table 1 ('AF' rows). The mean duration of the AF segments is from 6.93s (TT2) to 8.38s (TT3). The mean velocity of the animals in the AF segments ranged from 3.46 m/s (TT2) to 3.84 m/s (TT3), the mean power was between 800 W (TT1) to 925 W (TT3), and the minimum cost of transport was between 3.55 J/kg·m (TT2) and 5.07 J/kg·m (TT1).

A total of 277 consistent-speed segments were extracted from the swimming laps, Table 1 ('CS' rows). The mean duration of the CS segments is from 4.06s (TT2) to 4.19s (TT3). The mean velocity of the animals in the CS segments ranged from 3.73 m/s (TT2) to 4.22 m/s (TT3), the mean power was between 568 W (TT1) to 813 W (TT3), and the minimum cost of transport was between 2.30 J/kg·m (TT2) and 3.17 J/kg·m (TT1).

In Fig. 5, we observed that COTs of AF periods were significantly higher than CS periods in regular swimming intervals (0.5-5m/s). We compared the ratio of AF Min COT and CS Min COT for individuals. This ratio is from 1.71 (TT2) to 2.0 (TT3).

In Fig. 4 d) and Fig. 5 d), we clustered the data points from TT1-TT3 and conducted curve-fitting for $\widehat{P}_{\text{t,nd}} - v_{\text{bl}}$ and $\widehat{\text{COT}}_{\text{bl}} - v_{\text{bl}}$ correlations. We observed that the adjusted R^2 values of CS curve fitting is much better than the ones of AF period. That is because the AF periods accounted the energy cost for acceleration, which was not accounted in CS periods. The arbitrary acceleration, which caused arbitrary energy cost during AF periods, leads to worse R^2 values of the curve fitting.

We also observed that COTs of AF periods were significantly higher than CS periods in regular swimming intervals (0.5-5m/s). We compared the ratio of AF Min COT and CS Min COT for individuals. This ratio is from 1.71 (TT2) to 2.0 (TT3).

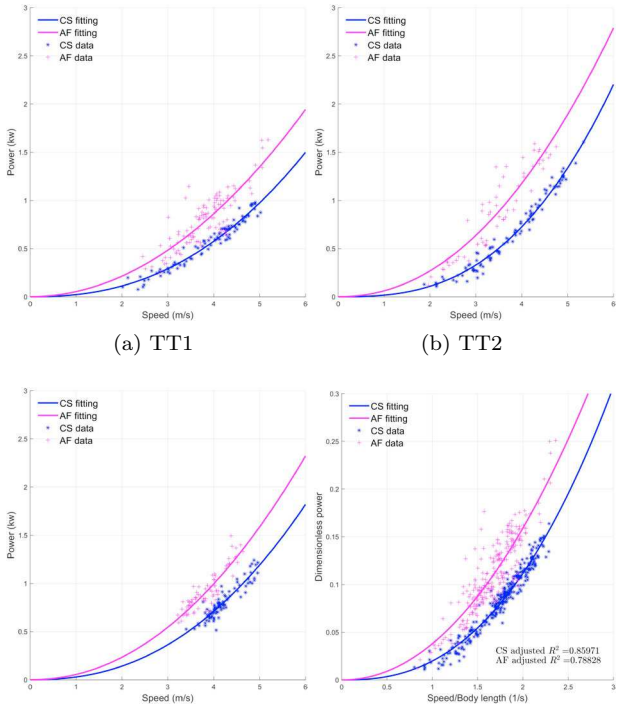

(a) TT1 (b) TT2

(c) TT3 (d) Overall

Fig. 4. Comparisons of speed vs power for AF segments (purple) and SS segments (blue) from existing literature (Gabaldon et al., 2022; Gabaldon, 2021). *TT1-3*: Subfigures a)-c) present the comparisons of animal speed vs thrust power. The experimental data and power-fitting are compared for TT1-3 individually in a)-c). *Overall*: Subfigure d) presents the comparison of body-speed vs non-dimensional thrust power. The experimental data from TT1-3 is clustered to conduct curve fitting between body-length speed and non-dimensional thrust power in d).

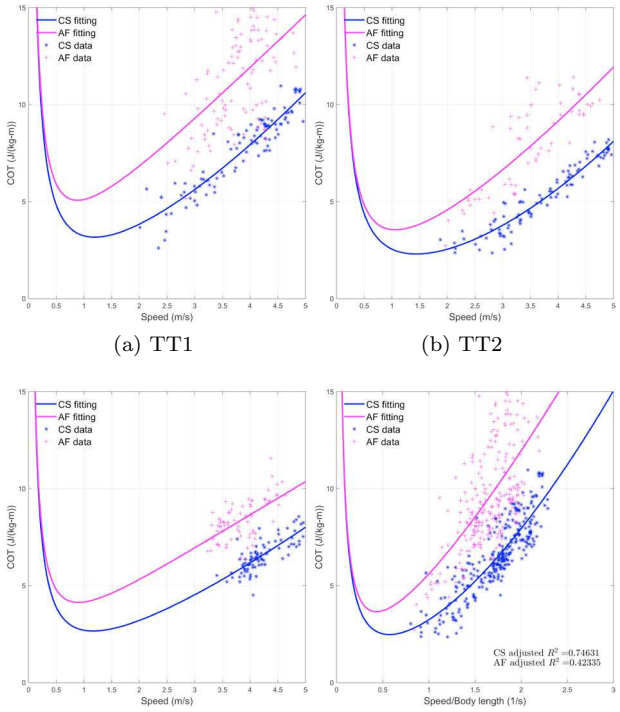

(a) TT1 (b) TT2

(c) TT3 (d) Overall

Fig. 5. Comparisons of speed vs COT for active fluking segments (purple) and constant speed swimming segments (blue) from existing literature (Gabaldon et al., 2022; Gabaldon, 2021). *TT1-3*: Subfigures a)-c) present the comparisons of animal speed vs COT. The experimental data and COT-fitting are compared for TT1-3 individually in a)-c). *Overall*: The experiment data from TT1-3 is clustered to conduct curve fitting between body length speed and COT in d).

4. CONCLUSION

In this article, we estimated the propulsive force generated during swimming locomotion using a simplified rigid body model of a dolphin and tag kinematic measurements. This approach enable the investigation of swimming biomechanics using hundreds of fluke strokes from one hundred and twenty laps of prescribed swimming. Animal specific models were created using parameters measured directly from the animals (mass, length, body diameter, fluke geometry) or estimated using published relationships between anthropometric measurements and the model parameter (animal volume and drag coefficient during low amplitude fluking). The prescribed swimming trials performed by the animals enabled an comparison between the cost to accelerate the animal to a given speed and those associated with overcoming the drag acting on the body at a constant swimming speed. These transient costs are significant, and increase as speed increases. For example, the average cost of transport for the period of active fluking was approximately 1.5 times larger than during constant speed swimming. Accounting for these transient costs will be important for future studies that use more direct measurements of metabolic cost (like respirometry) to verify estimates of energetic cost derived from measurements of kinematics.

REFERENCES

Allen, A.S., Read, A.J., Shorter, K.A., Gabaldon, J., Blawas, A.M., Rocho-Levine, J., and Fahlman, A. (2022). Dynamic body acceleration as a proxy to predict the cost of locomotion in bottlenose dolphins. *Journal of Experimental Biology*, 225(4), jeb243121.

Antoniak, G., Xargay, E., Gabaldon, J., Barton, K., Popa, B.I., and Shorter, K.A. (2023). Estimating propulsive efficiency of bottlenose dolphins during steady-state swimming. In *2023 IEEE Conference on Control Technology and Applications (CCTA)*, 675–680. IEEE.

Fahlman, A., Wilson, R., Svärd, C., Rosen, D.A., and Trites, A.W. (2008). Activity and diving metabolism correlate in steller sea lion eumetopias jubatus. *Aquatic Biology*, 2(1), 75–84.

Fish, F. and Lauder, G.V. (2006). Passive and active flow control by swimming fishes and mammals. *Annu. Rev. Fluid Mech.*, 38, 193–224.

	TT1	TT2	TT3	Overall
Mass (kg)	143	209	186	×
Length (m)	2.20	2.34	2.29	×
Radius (m)	0.20	0.23	0.21	×
RMR (W)	318	443	325	×
Lap count	54	29	37	120
AF count	108	58	73	239
CS count	97	95	85	277
AF Max vel. (m/s)	5.19	4.75	4.64	5.19
CS Max vel. (m/s)	5.02	5.35	4.96	5.35
AF Mean vel. (m/s)	3.81	3.46	3.84	3.74
CS Mean vel. (m/s)	3.88	3.73	4.22	3.94
AF Max power (kW)	1.63	1.59	1.50	1.63
CS Max power (kW)	0.98	1.61	1.24	1.61
AF Mean power (kW)	0.8	0.91	0.93	0.86
CS Mean power (kW)	0.57	0.67	0.81	0.68
AF Min COT (J/kg·m)	5.07	3.55	4.13	3.92
CS Min COT (J/kg·m)	3.17	2.30	2.66	2.63
Mean AF duration (s)	7.13	6.93	8.38	7.31
Mean CS duration (s)	4.07	4.06	4.19	4.11
AF a_1	53.39	61.45	54.94	64.77
AF a_2	2.01	2.13	2.09	1.95
CS a_1	21.81	16.28	28.34	19.03
CS a_2	2.36	2.74	2.32	2.56
AF a_1^*	0.04	0.04	0.04	0.04
AF a_2^*	2.01	2.13	2.09	2.07
CS a_1^*	0.03	0.03	0.03	0.03
CS a_2^*	2.07	2.14	2.07	2.06
c_1	0.24	0.43	0.39	×
c_2	-1.52	-1.38	-1.28	×
c_3	-0.004	0.0011	0.005	×
c_4	0.56	0.66	0.64	×

Table 1. The table presents measurements and summary parameters for periods of active-fluking (AF) and consistent swimming (CS) for the animals (TT 1–3). *(Top)*: Morphometric measurements of the animals. *(Middle)*: The statistical results of lap trial swimming. *(Bottom)*:Curve-fitting results of lap trial swimming. a_{1-2} and b_{1-2} are corresponding with curve-fitting results from the power vs speed curves and non-dimensional power vs body-length speed curves given by (4) and (5), respectively. c_{1-4} are corresponding with the efficiency vs speed coefficients presented in (7).

Fish, F.E. (1993). Power output and propulsive efficiency of swimming bottlenose dolphins (tursiops truncatus). *Journal of Experimental Biology*, 185(1), 179–193.

Fish, F.E. (1998). Comparative kinematics and hydrodynamics of odontocete cetaceans: morphological and ecological correlates with swimming performance. *Journal of Experimental Biology*, 201(20), 2867–2877.

Fish, F.E., Legac, P., Williams, T.M., and Wei, T. (2014). Measurement of hydrodynamic force generation by swimming dolphins using bubble dpiv. *Journal of Experimental Biology*, 217(2), 252–260.

Fish, F.E. and Rohr, J. (1999). Review of dolphin hydrodynamics and swimming performance.

Fossen, T.I. (2011). *Handbook of marine craft hydrodynamics and motion control*. John Wiley & Sons.

Gabaldon, J. (2021). *Contextualized Monitoring in the Marine Environment*. Ph.D. thesis.

Gabaldon, J.T., Zhang, D., Rocho-Levine, J., Moore, M.J., Van der Hoop, J., Barton, K., and Shorter, K.A. (2022). Tag-based estimates of bottlenose dolphin swimming behavior and energetics. *Journal of Experimental Biology*, 225(22), jeb244599.

Halsey, L.G., Green, J., Wilson, R., and Frappell, P. (2009). Accelerometry to estimate energy expenditure during activity: best practice with data loggers. *Physiological and Biochemical Zoology*, 82(4), 396–404.

Hertel, H. (1966). Structure form movement. *English Language Edition*.

Madgwick, S. et al. (2010). An efficient orientation filter for inertial and inertial/magnetic sensor arrays. *Report x-io and University of Bristol (UK)*, 25, 113–118.

Massaad, F., Lejeune, T.M., and Detrembleur, C. (2007). The up and down bobbing of human walking: a compromise between muscle work and efficiency. *The Journal of physiology*, 582(2), 789–799.

Schultz, W.W. and Webb, P.W. (2002). Power requirements of swimming: Do new methods resolve old questions? *Integrative and Comparative Biology*, 42(5), 1018–1025.

Tanaka, G., Yamane, T., Héroux, J.B., Nakane, R., Kanazawa, N., Takeda, S., Numata, H., Nakano, D., and Hirose, A. (2019). Recent advances in physical reservoir computing: A review. *Neural Networks*, 115, 100–123.

Van Der Hoop, J.M., Fahlman, A., Hurst, T., Rocho-Levine, J., Shorter, K.A., Petrov, V., and Moore, M.J. (2014). Bottlenose dolphins modify behavior to reduce metabolic effect of tag attachment. *Journal of Experimental Biology*, 217(23), 4229–4236.

Weihs, D. (2002). Dynamics of dolphin porpoising revisited. *Integrative and comparative biology*, 42(5), 1071–1078.

Williams, T.M., Friedl, W., and Haun, J. (1993). The physiology of bottlenose dolphins (tursiops truncatus): heart rate, metabolic rate and plasma lactate concentration during exercise. *Journal of experimental biology*, 179(1), 31–46.

Wilson, R.P., Börger, L., Holton, M.D., Scantlebury, D.M., Gómez-Laich, A., Quintana, F., Rosell, F., Graf, P.M., Williams, H., Gunner, R., et al. (2020). Estimates for energy expenditure in free-living animals using acceleration proxies: A reappraisal. *Journal of Animal Ecology*, 89(1), 161–172.

Wilson, R.P., White, C.R., Quintana, F., Halsey, L.G., Liebsch, N., Martin, G.R., and Butler, P.J. (2006). Moving towards acceleration for estimates of activity-specific metabolic rate in free-living animals: the case of the cormorant. *Journal of Animal Ecology*, 75(5), 1081–1090.

Xargay, E., Antoniak, G., Barton, K., and Shorter, K.A. (2023). A low-order model of dolphin swimming dynamics: fluke flexibility and energetics. In *2023 IEEE Conference on Control Technology and Applications (CCTA)*, 663–669. IEEE.

Yazdi, P., Kilian, A., and Culik, B. (1999). Energy expenditure of swimming bottlenose dolphins (tursiops truncatus). *Marine Biology*, 134, 601–607.